Title

Light-activated tetrazines enable precision live-cell bioorthogonal chemistry

Journal

Nature Chemistry, 14(9)

ISSN

1755-4330

Authors

Liu, Luping

Zhang, Dongyang

Johnson, Mai

et al.

Publication Date

2022-09-01

DOI

10.1038/s41557-022-00963-8

Peer reviewed

HHS Public Access

Author manuscript

Nat Chem. Author manuscript; available in PMC 2023 September 01.

Published in final edited form as:

Nat Chem. 2022 September ; 14(9): 1078–1085. doi:10.1038/s41557-022-00963-8.

Light-activated tetrazines enable precision live-cell bioorthogonal chemistry

Luping Liu,

Dongyang Zhang,

Mai Johnson,

Neal K. Devaraj✉

Department of Chemistry and Biochemistry, University of California, San Diego, CA, USA.

Abstract

Bioorthogonal cycloaddition reactions between tetrazines and strained dienophiles are widely used for protein, lipid and glycan labelling because of their extremely rapid kinetics. However, controlling this chemistry in the presence of living mammalian cells with a high degree of spatial and temporal precision remains a challenge. Here we demonstrate a versatile approach to light-activated formation of tetrazines from photocaged dihydrotetrazines. Photouncaging, followed by spontaneous transformation to reactive tetrazine, enables live-cell spatiotemporal control of rapid bioorthogonal cycloaddition with dienophiles such as *trans*-cyclooctenes. Photocaged dihydrotetrazines are stable in conditions that normally degrade tetrazines, enabling efficient early-stage incorporation of bioorthogonal handles into biomolecules such as peptides. Photocaged dihydrotetrazines allow the use of non-toxic light to trigger tetrazine ligations on living mammalian cells. By tagging reactive phospholipids with fluorophores, we demonstrate modification of HeLa cell membranes with single-cell spatial resolution. Finally, we show that photo-triggered therapy is possible by coupling tetrazine photoactivation with strategies that release prodrugs in response to tetrazine ligation.

Bioorthogonal ligations encompass coupling reactions that have considerable utility in living systems[1–3]. Among the numerous bioorthogonal reactions described so far, rapid inverse electron demand Diels–Alder reactions between tetrazines and dienophiles have found widespread use in chemical biology and material science since their introduction

✉**Correspondence and requests for materials** should be addressed to Neal K. Devaraj. ndevaraj@ucsd.edu.

Author contributions

L.L. and N.K.D. conceived the project. L.L. designed and performed the synthetic experiments. L.L. and D.Z. performed microscopy experiments. L.L. and M.J. performed cell experiments. L.L., D.Z., M.J. and N.K.D. analysed the data. L.L. and N.K.D. wrote the manuscript.

Online content

Any methods, additional references, Nature Research reporting summaries, source data, extended data, supplementary information, acknowledgements, peer review information; details of author contributions and competing interests; and statements of data and code availability are available at https://doi.org/10.1038/s41557-022-00963-8.

Competing interests

The authors declare no competing interests.

Supplementary information The online version contains supplementary material available at https://doi.org/10.1038/s41557-022-00963-8.

in 2008[4–7]. For example, tetrazine ligations have been used in whole-animal proteome labelling[8], the capture of circulating tumour cells[9], tracking lipid modifications[10] and imaging glycosylation[11]. In addition, dienophiles can cage a variety of functional groups, which are released after the cycloaddition reaction with tetrazine[12,13], and such 'click-to-release' strategies have been exploited for tumour imaging[14], controlling enzyme activity[15] and drug delivery[16]. Recently, tetrazine ligation-triggered drug delivery has entered human phase I clinical trials[17,18]. As applications rapidly expand, there is a growing need for methods that can precisely control the reaction in the presence of living cells. Because of its noninvasive nature and the high degree of spatial and temporal resolution attainable, light has become the tool of choice for remote manipulation of biological systems. For example, photoactivatable green fluorescent protein (GFP) has enabled numerous studies that track protein movement or mark specific cells in a population[19]. Similarly, light-controllable tetrazine ligations would open up applications such as cell surface engineering with single-cell precision and timed drug release[20]. Recent efforts toward engineering light-sensitive dienophiles such as caged cyclopropenes[21] and bicyclononynes[22] have enabled ultraviolet-light-induced tetrazine ligations with relatively modest reaction rates. However, ultraviolet light is toxic to living cells, particularly mammalian cells, which limits applications[23]. The *trans*-cyclooctenes (TCOs), the fastest reacting dienophiles, and caged click-to-release dienophiles have not yet been shown to be amenable to photocaging[24]. In principle, light-triggered tetrazine formation would circumvent these issues. A visible-light-triggered oxidation of 1,4-dihydrotetrazines to tetrazines using photosensitizers has been developed[25]. However, photosensitizers such as methylene blue can be toxic, and the use of a diffusible mediator limits spatiotemporal control[26]. We hypothesized that activation of photocaged tetrazines using light would address these challenges and facilitate precision chemistry in biological systems.

Results

To develop a light-triggered tetrazine ligation with high spatiotemporal precision, we explored whether a tetrazine precursor could be caged by a photoprotecting group (Fig. 1a). Dihydrotetrazine is unreactive to dienophiles[25] and can be oxidized in air to form tetrazine[24]. Therefore, we asked whether the secondary amines of dihydrotetrazine could be modified with light-cleavable protecting groups, such as nitrophenyl derivatives[27]. Photocaging would prevent the oxidation of dihydrotetrazine to tetrazine, creating a compound that is inactive to cycloaddition with strained dienophiles. The caging group would be removed upon exposure to light, leading to the formation of tetrazine after a subsequent oxidation reaction. The in situ formed tetrazine would be able to react rapidly with a dienophile through inverse electron demand Diels–Alder cycloaddition. By directly activating the tetrazine, spatial control could be achieved.

Synthesis of photocaged tetrazine precursors.

A photocaged dihydrotetrazine should be stable in aqueous solution, and the product of decaging should be rapidly oxidized to tetrazine. With these conditions in mind, we synthesized photocaged dihydrotetrazine **1a** from 3-(but-3-yn-1-yl)-6-phenyl-1,2,4,5-tetrazine, which could be converted to the corresponding dihydrotetrazine using the

reductant thiourea dioxide (Fig. 1b). 1-(2-Nitrophenyl)ethyl carbamate was chosen as the photocleavable functional group due to its sensitivity to light[28] and biocompatibility[29]. After reacting the dihydrotetrazine with the selected photocleavable group, the desired product 1-(2-nitrophenyl)ethyl-6-(but-3-yn-1-yl)-3-phenyl-1,2,4,5-tetrazine-1(4*H*)-carboxylate photocaged dihydrotetrazine **1a** was obtained. NMR studies confirmed that the secondary amine adjacent to the alkyl group of dihydrotetrazine **1a** is functionalized (Supplementary NMR spectra of **1a**). After analysing the absorbance spectrum of photocaged dihydrotetrazine **1a** (Supplementary Fig. 1a), a 405-nm-centred light-emitting diode (LED) light (see Supplementary Fig. 2 for full emission spectra of the employed LED lights) was chosen to trigger tetrazine formation (Fig. 1c and Supplementary Fig. 3). HPLC revealed that 94% of **1a** (16 μM) was decaged when irradiated with LED light (405 nm, 18 W) for 2 min under open air at 37 °C in aqueous buffer (phosphate buffered saline (PBS) containing 0.1% dimethyl sulfoxide (DMSO)). A 74% yield of tetrazine **2a** was immediately formed. These results are comparable to the yields of reactive species formed from alternative popular photo-activated bioconjugation reactions such as tetrazole photoclick chemistry[30].

As discussed, we initially speculated that a dihydrotetrazine intermediate would be formed after light activation, which would then be spontaneously oxidized to tetrazine by oxygen. To test this hypothesis we investigated the oxidation reaction of 3-(but-3-yn-1-yl)-6-phenyl-1,4-dihydro-1,2,4,5-tetrazine under the same conditions (Supplementary Fig. 4). To our surprise, only a minor amount of tetrazine **2a** was detectable after irradiating 3-(but-3-yn-1-yl)-6-phenyl-1,4-d ihydro-1,2,4,5-tetrazine **S1a** (16 μM) with LED light (405 nm, 18 W) for 2 min under open air at 37 °C in aqueous buffer (PBS containing 0.1% DMSO) (Supplementary Fig. 4a). Instead, it took 9 h to obtain a 70% yield of tetrazine **2a** by oxidizing dihydrotetrazine **S1a** in air (Supplementary Fig. 4b). These results suggest that dihydrotetrazine is not the key intermediate in the light-activated formation of tetrazine. Although speculative, it is possible that light activation generates an active intermediate 3-(but-3-yn-1-yl)-6-phenyl-1*H*-1,2,4,5-tetrazin-4-ide (Fig. 1c)[31], which is directly oxidized to tetrazine **2a**.

Our findings encouraged us to further explore the substrate scope for photoactivation. We decided to explore the suitability of various photoprotecting groups and whether alternative substituents on the dihydrotetrazine were tolerated (Table 1, **1a**–**1h**). We successfully incorporated redshifted light-cleavable protecting groups such as a 6-nitropiperonyl methyl photocage (Table 1, **1b**, cleavable with 425-nm-centred LED light) and a diethylaminocoumarin photocage (Table 1, **1c**, cleavable with 450-nm-centred LED light) onto 3-(but-3-yn-1-yl)-6-phenyl-1,4-dihydro-1,2,4,5-te trazine and characterized their absorbance spectra (Supplementary Fig. 1). Tetrazine **2a** was obtained in 58–74% yields by irradiating photocaged dihydrotetrazines (Table 1, **1a**–**1c**) with the appropriate LED light in PBS solution (Supplementary Figs. 3, 5 and 6). We also explored different substituents on the dihydrotetrazines as tetrazine substituents can greatly affect the reaction rate of cycloaddition with dienophiles (Table 1, **1d**–**1h** and Supplementary Figs. 7–11). Specifically, we sought to see if photouncaging could enable access to more electron-deficient tetrazines, as such tetrazines are expected to react more rapidly

with dienophiles. For example, we found that 3,6-diphenyl-1,2,4,5-tetrazine **2b** could be generated from diethylaminocoumarin photoprotected dihydrotetrazine **1d** (63% yield after irradiation with LED light, 450 nm, 18 W, 2 min) and from 6-nitropiperonyl methyl photoprotected dihydrotetrazine **1g** (60% yield after irradiation with LED light, 405 nm, 18 W, 2 min) in PBS solution under open air at 37 °C (Supplementary Figs. 7 and 10). Interestingly, electron-deficient dipyridyl-substituted tetrazine **2e** was accessible from photocaged dihydrotetrazine **1h** through the photouncaging approach (60% yield after irradiation with LED light, 405 nm, 18 W, for 3 min; Supplementary Fig. 11). Electron-poor tetrazines with dipyridyl substituents have been reported to react with ring-strained *trans*-cyclooctene dienophiles at extraordinarily high reaction rates ($>10^6$ M^{-1} s^{-1})[32]. Finally, we also explored the synthesis of a boron-dipyrromethene (BODIPY) photocaged dihydrotetrazine[33]. Although reactions were low yielding, trace amounts of the desired photocaged product were obtained (Supplementary Fig. 12). Preliminary results demonstrated that photouncaging with 525-nm-centred green LED light led to the formation of tetrazine **2a** (Supplementary Fig. 13). Future optimization of synthetic protocols will probably be required for practical applications and will further broaden the substrate scope of dihydrotetrazine photocaging.

The stability of the photocaged dihydrotetrazines in aqueous media was characterized and compared to the tetrazine products. **1a** (precursor of tetrazine **2a**) and **1h** (precursor of dipyridyl-substituted tetrazine **2e**) were selected because of their differing substituents. In the absence of light, degradation of **1a** was not observed in either PBS or cell lysate at 37 °C over 24 h (Supplementary Fig. 14). Under the same conditions, less than 1% degradation in PBS and ~5% degradation in cell lysate was detected for **1h** (Supplementary Fig. 15). These results demonstrate the high stability of photocaged dihydrotetrazines in biologically relevant aqueous solutions in the absence of irradiation. In comparison, we also examined the stability of the corresponding tetrazines **2a** and **2e** under the same conditions. Although 3-(but-3-yn-1-yl)-6-phenyl-1,2,4,5-tetrazine **2a** was stable in PBS or cell lysate at 37 °C over 24 h (Supplementary Fig. 16), tetrazine **2e** with electron-withdrawing dipyridyl substituents turned out to be highly susceptible to degradation in aqueous solutions (Supplementary Fig. 17). In the absence of irradiation, 25% and 73% of tetrazine **2e** degraded in PBS at 37 °C over 6 h and 24 h, respectively. In cell lysate at 37 °C, we observed 57% and 100% degradation of **2e** over 6 h and 24 h, respectively. Therefore, our methodology of light-activated generation of **2e** from stable photocaged dihydrotetrazine **1h** could address the poor stability of electron-deficient tetrazines in aqueous solution, and it will be important to find the appropriate balance between the stability and reactivity of electron-poor tetrazines depending on the intended application. As expected, reaction between the caged dihydrotetrazine and a model strained dienophile, the axial isomer of *trans*-4-cycloocten-1-ol (TCO-OH), did not occur in the absence of light (Supplementary Fig. 18). In addition, we measured a second-order rate constant of 101 ± 3 M^{-1} s^{-1} between **2a** and the axial isomer of TCO-OH at 20 °C in PBS solution (containing 10% DMSO), by monitoring the disappearance of the characteristic tetrazine visible absorption at 521 nm under pseudo first-order conditions (Supplementary Fig. 19)[13].

Functionalization of peptides with bioorthogonal handles.

Having synthesized various photocaged dihydrotetrazines that can be activated by light, we next explored specific bioconjugation applications. A drawback of tetrazines can be their susceptibility to degradation, particularly in the presence of nucleophiles and base[34,35]. This feature has hampered conjugation applications, particularly if tetrazines are required to be stable in physiological media for lengthy periods of time before cycloaddition, such as for pretargeted imaging, drug delivery applications or in cases where early-stage modification of tetrazine is desired. For example, although tetrazine ligations have been widely used to modify peptides, the tetrazine is typically introduced in the late stage of peptide synthesis due to its incompatibility with solid-phase peptide synthesis (SPPS) reaction conditions[36]. Electron-poor tetrazine-containing amino acids are not used in Fmoc solid-phase peptide synthesis (SPPS) due to their degradation during the standard repeated Fmoc deprotection conditions (for example, 4-methylpiperidine/dimethylformamide (DMF)).

Considering the stability of photocaged dihydrotetrazines, we asked whether such groups could act as photoprotection moieties, masking latent tetrazines through harsh conditions that would normally be degradative. For example, in 4-methylpiperidine/DMF solution, 40% of tetrazine **2a** degrades in 30 min (Supplementary Fig. 20). By contrast, photocaged dihydrotetrazine **1a** is stable in 4-methylpiperidine/DMF solution with no detectable degradation observed under the same reaction conditions. We thus speculated that photocaged dihydrotetrazines would be tolerated during SPPS. To test this, we synthesized unnatural Fmoc-protected amino acid **1i** containing a photocaged dihydrotetrazine (Supplementary Fig. 21). We employed **1i** in SPPS to obtain a five-amino-acid peptide **1j** in 50% yield (Supplementary Fig. 22). After LED irradiation of photocaged dihydrotetrazine peptide **1j** (10 μM) for 2 min in PBS at 37 °C, tetrazine peptide **2f** was formed in 96% conversion (Fig. 2b). Being able to directly use photoprotected tetrazine amino acids facilitates SPPS of peptides that contain multiple bioorthogonal handles, such as an azido group and tetrazine (Supplementary Fig. 23), making it easier to site-specifically label peptides with multiple probes (Supplementary Fig. 24).

Single-cell remodelling of cell membranes.

Because our strategy utilizes visible light to directly generate tetrazines from their precursors, we asked whether photocaged dihydrotetrazines could spatio-temporally modify living cells, for example, by covalently labelling membrane lipids (Fig. 3a). Modified synthetic phospholipids have seen extensive use for tagging cellular membranes[37,38]. To remodel cell membranes with photocaged dihydrotetrazines, we appended **1a** to a derivative of 1,2-dipalmitoyl-*sn*-glycero-3-phosphoethanolamine (DPPE) to form photocaged dihydrotetrazine-diacylphospholipid **1k** (Fig. 3b and Supplementary Fig. 25). On irradiation with LED light (405 nm, 18 W), **1k** reacted rapidly with a water-soluble *trans*-cyclooctene modified Alexa Fluor 488 dye (TCO-AF488) **3a**, forming cycloaddition product **4a**, as determined by liquid chromatography mass spectrometry (LC-MS; Supplementary Fig. 26). Encouraged by earlier reports of using 405-nm laser sources to activate 1-(2-nitrophenyl)ethyl cages, we next tested whether **1k** would enable spatiotemporal labelling of live cells[39]. To incorporate photocaged dihydrotetrazine onto cell membranes, adherent HeLa S3 cells were incubated with 60 nM photocaged

dihydrotetrazine-diacylphospholipid **1k** in PBS solution (containing 0.1% DMSO) at 37 °C for 5 min. Excess **1k** was removed by washing cells with PBS solution. The washed cells were then incubated with 3 nM TCO-AF488 **3a** in PBS solution (containing 0.1% DMSO). To trigger in situ formation of tetrazine and the subsequent bioorthogonal tetrazine ligation, a single cell among a population of cells was selectively irradiated with a 405-nm laser (20 mW) for 20 s using a ZEISS 880 laser scanning microscope. Five minutes after the laser uncaging event, unreacted TCO-AF488 was removed by exchanging the solution with fresh cell culture medium. Fluorescence live-cell imaging was performed to reveal whether tetrazine ligation had taken place on the membrane of the laser-irradiated cell. Fluorescence labelling by AF488 was only observed on the membrane of the laser-irradiated cell and not on adjacent cells, illustrating that precise spatiotemporal photoactivation of tetrazine ligation can be achieved using photocaged dihydrotetrazine-diacylphospholipid **1k** (Fig. 3c).

To demonstrate the versatility of the light-activated single-cell manipulation, we also performed labelling with an alternative TCO-modified dye, Alexa Fluor 568 (TCO-AF568) **3b** (Fig. 3d and Supplementary Fig. 28). Additionally, our technique can be applied to other types of mammalian cell, such as Hep 3B human liver cancer cells (Supplementary Fig. 29). Finally, to test the robustness of spatial photoactivation, populations of one or two cells located at four different locations inside a 0.75 mm by 0.75 mm area were selectively laser-irradiated at 405 nm to trigger tetrazine ligation, modifying the associated cell membranes (Fig. 3e). Fluorescence labelling was only observed on the laser-irradiated cells, demonstrating that reliable spatiotemporal labelling of living cells can be achieved by photoactivation of surface tetrazines.

Light-activated drug delivery.

An application of tetrazine ligation is the so-called click-to-release strategy, which typically involves utilizing a dienophile to cage a bioactive molecule such as a drug[24]. Upon reaction with tetrazine, tautomerization of the cycloadduct occurs, leading to elimination and drug release[12]. We speculated that combining light-activated tetrazine formation with click-to-release strategies would facilitate the controlled release of therapeutics in the presence of living systems for photopharmacology. To couple light-activated tetrazine ligation with click to release, we synthesized a dienophile-modified prodrug, TCO carbamate-caged doxorubicin **3c** (TCO-Dox; Supplementary Fig. 30), which liberates doxorubicin **5a** (Dox) after undergoing a cycloaddition reaction with tetrazine (Fig. 4a). Doxorubicin is an anticancer drug, and we therefore sought to use light to stimulate doxorubicin delivery to cancer cells through a dual activation process (Fig. 4a), triggering apoptosis. Initial experiments were performed using nitrophenyl photocaged dihydrotetrazine **1a**, and light-activated tetrazine drug release was successfully achieved in vitro and in cellulo with 405-nm-centred LED light (Supplementary Figs. 31–34). To improve the biocompatibility of the approach, we explored the use of the more redshifted coumarin photocaged dihydrotetrazine **1c** to achieve release of the chemotherapeutic doxorubicin in the presence of living Hep 3B cancer cells using 450-nm-centred LED light (Fig. 4). As shown in Fig. 4b, when Hep 3B human liver cancer cells were treated with a mixture of diethylaminocoumarin photocaged dihydrotetrazine **1c** (8 μM) and TCO-Dox **3c** (5.5 μM), no decrease in cell viability was observed compared to untreated cells. However, on irradiation with LED light (450 nm, 18

W) for 2 min, followed by incubation for 24 h, a 57 ± 2% reduction in cell viability was observed. The loss of cell viability was similar to that observed when cells were directly treated with Dox **5a** (5.5 μM) under the same conditions. There was no influence on cell viability when cells were irradiated with LED light for 2 min in the presence of either photocaged dihydrotetrazine **1a** (8 μM), TCO-Dox **3c** (5.5 μM) or side product **4c** (5.5 μM) alone. These results demonstrate that photocaged dihydrotetrazines can be utilized for the light-triggered release of bioactive compounds, such as chemotherapeutics, in the presence of living cells.

Discussion

Here we have demonstrated a methodology for the photoactivation of tetrazines that enables biomolecular labelling, spatiotemporal modification of live-cell membranes with single-cell precision and photopharmacology when combined with click-to-release strategies. Tetrazine instability is a well-recognized obstacle to their use, and we have found that photocaged tetrazine precursors are highly stable, even in the presence of the strong bases that rapidly degrade tetrazines. Given the stability of photocaged dihydrotetrazines, we expect they will find broad application as a general tetrazine protecting group. Photocaged dihydrotetrazines would be especially useful in conditions known to degrade tetrazines, such as those encountered during the installation of ^{18}F radionuclides for PET imaging[34], or for live-cell pulse-chase experiments where tetrazine reactivity would be required to be maintained for an arbitrary amount of time before reaction[40]. Indeed, preliminary results indicate that photocaged dihydrotetrazines, unlike tetrazines, are very stable under the conditions typically used for fluorination (Supplementary Fig. 35). Because our method uses light to activate caged tetrazine precursors, high spatiotemporal precision is achievable. By modifying phospholipids on cell surfaces, we showed that single-cell activation is feasible. The technique could enable monitoring of lipid trafficking and dynamics in living cells by controlling where and when caged tetrazines on lipids are activated and following their transport by post-labelling with dienophile-modified fluorophores, although there would be a delay before imaging can take place to remove excess unreacted fluorophore[41]. Such a delay might be avoided by the future use of fluorogenic dienophiles that could react with tetrazines and are compatible with live-cell labelling[42]. Light-activated release of the chemotherapeutic doxorubicin was carried out by combining photoactivation of tetrazine formation with ‘click to release’ strategies. The photocaged tetrazine precursor and light alone showed negligible toxicity, demonstrating the biocompatibility of the technique. Such optically controlled drug release may have practical applications in image-guided surgery and photodynamic therapy[43]. Future studies will explore alternative caging groups that activate in response to even longer wavelengths of light, enabling multiplexing and facilitating in vivo studies[27]. The basic concept we present might also be extended to other amine caging functionalities capable of masking dihydrotetrazines, allowing rapid biorthogonal ligation in response to additional stimuli, such as enzymatic activity, pH or the presence of metal complexes[44,45].

Methods

Synthesis of photocaged dihydrotetrazine.

General procedure to prepare 1-(2-nitrophenyl)ethyl-6-(but-3-yn-1-yl)-3-phenyl-1,2,4,5-tetrazine-1(4*H*)-carboxylate **1a**: in a sealed flask, the reductant thiourea dioxide (160 mg, 1.5 mmol) was added to a solution of tetrazine **2a** (210 mg, 1.0 mmol) in 7.5 ml of DMF/H_2O (vol/vol = 10/1) at room temperature under argon. The reaction mixture was stirred in an oil bath at 95 °C for 1 h. On completion, the colour of the reaction mixture changed from pink to light yellow. The reaction solvent was removed under reduced pressure and the residue was dried under high vacuum overnight, resulting in a powder containing dihydrotetrazine, which was transferred to a sealed flask under argon and directly used for the next step. Under argon, 15 ml of anhydrous pyridine was added, followed by slow addition of a solution of 1-(2-nitrophenyl)ethyl carbonochloridate (532 mg, 2.3 mmol) in toluene (2.5 ml) at room temperature. The reaction mixture was stirred at 95 °C for 24 h. On completion, the reaction mixture was concentrated under reduced pressure. The residue was purified by column chromatography on silica gel using 50–100% CH_2Cl_2/hexane to 15% MeOH/CH_2Cl_2 as the eluents, yielding the title compound **1a** as a pale-yellow solid (263 mg, 65%). Full experimental details and characterization of the newly described compounds are provided in the Supplementary Information.

Single-cell remodelling of cell membranes.

Human HeLa S3 cancer cells (ATCC, CCL-2.2) were grown in the complete medium Dulbecco's modified Eagle's minimal essential medium (DMEM) with high glucose (Life Technologies–Gibco, 11995073) supplemented with 10% heat-inactivated fetal bovine serum (FBS; Omega Scientific, FB02), 100 U ml^{-1} penicillin and 100 μg ml^{-1} streptomycin (Life Technologies–Gibco, 15140122). Cells were grown at 37 °C in a humidified atmosphere containing 5% CO_2. An eight-well chamber slide (cat. no. 80826, ibidi USA) was pre-coated with 0.5% (wt/vol) poly-lysine in H_2O to facilitate cell adhesion during imaging. HeLa S3 cell lines were plated at 40% density per well on eight-well plates in 200 μl of DMEM complete medium. After 24 h, the cells were treated as follows. HeLa S3 cancer cells were incubated in 200 μl of photocaged dihydrotetrazine-diacylphospholipid **1k** (60 nM) in PBS solution (containing 0.1% DMSO) at 37 °C for 5 min. Excess **1k** was then removed by washing the cells with fresh PBS solution. Next, the washed cells were incubated with 3 nM TCO-modified Alexa Fluor in PBS solution (containing 0.1% DMSO). To trigger the activation of the photocaged dihydrotetrazine and the subsequent bioorthogonal tetrazine ligation, selected cells were laser-irradiated (405 nm, 20 mW) for 20 s using a ZEISS 880 laser scanning microscope. Five minutes after the laser uncaging event, the cells were washed with fresh full-growth medium and were imaged by fluorescence microscopy.

Light-activated drug delivery.

Human Hep 3B hepatocellular carcinoma cells (ATCC, HB-8064) were grown in the complete medium Eagle's minimal essential medium (EMEM) with high glucose (Life Technologies–Gibco, 11995073) supplemented with 10% heat-inactivated FBS (Omega Scientific, FB02), 100 U ml^{-1} penicillin and 100 μg ml^{-1} streptomycin (Life Technologies–

Gibco, 15140122). Cells were grown at 37 °C in a humidified atmosphere containing 5% CO_2. Hep 3B cell lines were plated at 30,000 cells per well on 96-well plates in 200 μl of EMEM complete medium and incubated for 24 h to promote cell adhesion and growth. The cells were then treated, respectively, with photocaged dihydrotetrazine **1c** (8 μM), TCO-Dox **3c** (5.5 μM), side product **4c** (5.5 μM) and Dox **5a** (5.5 μM), with or without irradiation by LED light (450 nm, 18 W) for 2 min, followed by incubation at 37 °C for 24 h. Cell viability assays of Hep 3B cancer cells were carried out next.

ATCC has profiled cell lines using polymorphic short tandem repeat (STR) loci (TH01, TPOX, vWA, CSF1PO, D16S539, D7S820, D13S317 and D5S818) plus amelogenin for gender identification.

Statistics and reproducibility.

Statistically significant differences in cell viability in Fig. 4b between no treatment and other treatments are indicated using an independent *t*-test (two-tailed): ***$P < 0.001$; NS, not significant. Specifically, **1c** + **3c** (450-nm irradiation) versus no treatment: $t = 10.334$, d.f. = 4, $P = 0.000495$; **5a** (450-nm irradiation) versus no treatment: $t = 10.755$, d.f. = 4, $P = 0.000424$, 95% confidence interval is 41.51–72.01.

Statistically significant differences in cell viability in Supplementary Fig. 34b between no treatment and other treatments are indicated using an independent *t*-test (two-tailed): ***$P < 0.001$; NS, not significant. Specifically, **1a** + **3c** (405-nm irradiation) versus no treatment: $t = 11.038$, d.f. = 4, $P = 0.000383$; **5a** (450-nm irradiation) versus no treatment: $t = 11.691$, d.f. = 4, $P = 0.000306$, 95% confidence interval is 56.26–91.31.

Reporting summary.

Further information on research design is available in the Nature Research Reporting summary linked to this Article.

Supplementary Material

Refer to Web version on PubMed Central for supplementary material.

Acknowledgements

Financial support for this work was provided by the National Institutes of Health (DP2DK111801, R01GM123285, R35GM141939 and T32CA009523). We thank W. Xiong and C. Wang for their assistance in measuring the emission spectra of the LED lights. We thank A. Winter and E. Gehrmann for their assistance with the synthesis of BODIPY photocaged dihydrotetrazine. We thank I. Budin and G. Riddihough for providing helpful comments.

Data availability

The data that support the findings of this study are available within the paper and its Supplementary Information. Source data are provided with this paper.

References

1. Saxon E & Bertozzi CR Cell surface engineering by a modified Staudinger reaction. Science 287, 2007–2010 (2000). [PubMed: 10720325]
2. Prescher JA, Dube DH & Bertozzi CR Chemical remodelling of cell surfaces in living animals. Nature 430, 873–877 (2004). [PubMed: 15318217]
3. Devaraj NK The future of bioorthogonal chemistry. ACS Cent. Sci 4, 952–959 (2018). [PubMed: 30159392]
4. Blackman ML, Royzen M & Fox JM Rapid tetrazine ligation: fast bioconjugation based on inverse-electron-demand Diels–Alder reactivity. J. Am. Chem. Soc 130, 13518–13519 (2008). [PubMed: 18798613]
5. Devaraj NK, Weissleder R & Hilderbrand SA Tetrazine-based cycloadditions: application to pretargeted live cell imaging. Bioconjug. Chem 19, 2297–2299 (2008). [PubMed: 19053305]
6. Oliveira BL, Guo Z & Bernardes GJL Inverse electron demand Diels-Alder reactions in chemical biology. Chem. Soc. Rev 46, 4895–4950 (2017). [PubMed: 28660957]
7. Nguyen SS & Prescher JA Developing bioorthogonal probes to span a spectrum of reactivities. Nat. Rev. Chem 4, 476–489 (2020). [PubMed: 34291176]
8. Elliott TS et al. Proteome labeling and protein identification in specific tissues and at specific developmental stages in an animal. Nat. Biotechnol 32, 465–472 (2014). [PubMed: 24727715]
9. Dong J et al. Covalent chemistry on nanostructured substrates enables noninvasive quantification of gene rearrangements in circulating tumor cells. Sci. Adv 5, eaav9186 (2019). [PubMed: 31392269]
10. Liang D et al. A real-time, click chemistry imaging approach reveals stimulus-specific subcellular locations of phospholipase D activity. Proc. Natl Acad. Sci. USA 116, 15453–15462 (2019). [PubMed: 31311871]
11. Agarwal P, Beahm BJ, Shieh P & Bertozzi CR Systemic fluorescence imaging of zebrafish glycans with bioorthogonal chemistry. Angew. Chem. Int. Ed 54, 11504–11510 (2015).
12. Carlson JCT, Mikula H & Weissleder R Unraveling tetrazine-triggered bioorthogonal elimination enables chemical tools for ultrafast release and universal cleavage. J. Am. Chem. Soc 140, 3603–3612 (2018). [PubMed: 29384666]
13. Versteegen RM et al. Click-to-release from *trans*-cyclooctenes: mechanistic insights and expansion of scope from established carbamate to remarkable ether cleavage. Angew. Chem. Int. Ed 57, 10494–10499 (2018).
14. Li H, Conde J, Guerreiro A & Bernardes GJL Tetrazine carbon nanotubes for pretargeted in vivo ‘click-to-release’ bioorthogonal tumour imaging. Angew. Chem. Int. Ed 59, 16023–16032 (2020).
15. Li J, Jia S & Chen PR Diels–Alder reaction-triggered bioorthogonal protein decaging in living cells. Nat. Chem. Biol 10, 1003–1005 (2014). [PubMed: 25362360]
16. Ji X et al. Click and release: bioorthogonal approaches to ‘on-demand’ activation of prodrugs. Chem. Soc. Rev 48, 1077–1094 (2019). [PubMed: 30724944]
17. Czuban M et al. Bio-orthogonal chemistry and reloadable biomaterial enable local activation of antibiotic prodrugs and enhance treatments against *Staphylococcus aureus* infections. ACS Cent. Sci 4, 1624–1632 (2018). [PubMed: 30648146]
18. Wu K et al. Click activated protodrugs against cancer increase the therapeutic potential of chemotherapy through local capture and activation. Chem. Sci 12, 1259–1271 (2021). [PubMed: 34163888]
19. Patterson GH & Lippincott-Schwartz J A photoactivatable GFP for selective photolabeling of proteins and cells. Science 297, 1873–1887 (2002). [PubMed: 12228718]
20. Kumar GS & Lin Q Light-triggered click chemistry. Chem. Rev 121, 6991–7031 (2021). [PubMed: 33104332]
21. Kumar P, Jiang T, Li S, Zainul O & Laughlin ST Caged cyclopropenes for controlling bioorthogonal reactivity. Org. Biomol. Chem 16, 4081–4085 (2018). [PubMed: 29790564]
22. Mayer SV, Murnauer A, von Wrisberg MK, Jokisch ML & Lang K Photo-induced and rapid labeling of tetrazine-bearing proteins via cyclopropenone-caged bicyclononynes. Angew. Chem. Int. Ed 58, 15876–15882 (2019).

23. Hockberger PE A history of ultraviolet photobiology for humans, animals and microorganisms. Photochem. Photobiol 76, 561–579 (2002). [PubMed: 12511035]
24. Versteegen RM, Rossin R, ten Hoeve W, Janssen HM & Robillard MS Click to release: instantaneous doxorubicin elimination upon tetrazine ligation. Angew. Chem. Int. Ed 52, 14112–14116 (2013).
25. Zhang H et al. Rapid bioorthogonal chemistry turn-on through enzymatic or long wavelength photocatalytic activation of tetrazine ligation. J. Am. Chem. Soc 138, 5978–5983 (2016). [PubMed: 27078610]
26. da Costa SR, da Costa Monteiro M, da Silva Júnior FMR & Sandrini JZ Methylene blue toxicity in zebrafish cell line is dependent on light exposure. Cell Biol. Int 40, 895–905 (2016). [PubMed: 27238358]
27. Hansen MJ, Velema WA, Lerch MM, Szymanski W & Feringa BL Wavelength-selective cleavage of photoprotecting groups: strategies and applications in dynamic systems. Chem. Soc. Rev 44, 3358–3377 (2015). [PubMed: 25917924]
28. Corrie JET, Barth A, Munasinghe VRN, Trentham DR & Hutter MC Photolytic cleavage of 1-(2-nitrophenyl)ethyl ethers involves two parallel pathways and product release is rate-limited by decomposition of a common hemiacetal intermediate. J. Am. Chem. Soc 125, 8546–8554 (2003). [PubMed: 12848562]
29. Zhao YR et al. New caged coumarin fluorophores with extraordinary uncaging cross sections suitable for biological imaging applications. J. Am. Chem. Soc 126, 4653–4663 (2004). [PubMed: 15070382]
30. An P, Lewandowski TM, Erbay TG, Liu P & Lin Q Sterically shielded, stabilized nitrile imine for rapid bioorthogonal protein labeling in live cells. J. Am. Chem. Soc 140, 4860–4868 (2018). [PubMed: 29565582]
31. Walker JW, Reid GP, McCray JA & Trentham DR Photolabile 1-(2-nitrophenyl) ethyl phosphate esters of adenine nucleotide analogs. Synthesis and mechanism of photolysis. J. Am. Chem. Soc 110, 7170–7177 (1988).
32. Darko A et al. Conformationally strained *trans*-cyclooctene with improved stability and excellent reactivity in tetrazine ligation. Chem. Sci 5, 3370–3776 (2014).
33. Slanina T et al. In search of the perfect photocage: structure–reactivity relationships in meso-methyl BODIPY photoremovable protecting groups. J. Am. Chem. Soc 139, 15168–15175 (2017). [PubMed: 29039200]
34. Li Z et al. Tetrazine-*trans*-cyclooctene ligation for the rapid construction of ^{18}F labeled probes. Chem. Commun 46, 8043–8045 (2010).
35. Selvaraj R et al. Tetrazine-*trans*-cyclooctene ligation for the rapid construction of integrin $\alpha_v\beta_3$ targeted PET tracer based on a cyclic RGD peptide. Bioorg. Med. Chem. Lett 21, 5011–5014 (2011). [PubMed: 21601452]
36. Pagel M Inverse electron demand Diels-Alder (IEDDA) reactions in peptide chemistry. J. Pept. Sci 25, e3141 (2019). [PubMed: 30585397]
37. Jin C et al. Phosphorylated lipid-conjugated oligonucleotide selectively anchors on cell membranes with high alkaline phosphatase expression. Nat. Commun 10, 2704 (2019). [PubMed: 31221964]
38. Huang ML, Smith RA, Trieger GW & Godula K Glycocalyx remodeling with proteoglycan mimetics promotes neural specification in embryonic stem cells. J. Am. Chem. Soc 136, 10565–10568 (2014). [PubMed: 25019314]
39. Trigo FF, Corrie JET & Ogden D Laser photolysis of caged compounds at 405 nm: photochemical advantages, localisation, phototoxicity and methods for calibration. J. Neurosci. Methods 180, 9–21 (2009). [PubMed: 19427524]
40. Willis JCW & Chin JW Mutually orthogonal pyrrolysyl-tRNA synthetase/tRNA pairs. Nat. Chem 10, 831–837 (2018). [PubMed: 29807989]
41. Tamura T et al. Organelle membrane-specific chemical labeling and dynamic imaging in living cells. Nat. Chem. Biol 16, 1361–1367 (2020). [PubMed: 32958953]
42. Jewett JC & Bertozzi CR Synthesis of a fluorogenic cyclooctyne activated by Cu-free click chemistry. Org. Lett 13, 5937–5939 (2011). [PubMed: 22029411]

43. Kwiatkowski S et al. Photodynamic therapy—mechanisms, photosensitizers and combinations. Biomed. Pharmacother 106, 1098–1107 (2013).

44. Cao Z et al. pH- and enzyme-triggered drug release as an important process in the design of anti-tumor drug delivery systems. Biomed. Pharmacother 118, 109340 (2019). [PubMed: 31545284]

45. Li J et al. Palladium-triggered deprotection chemistry for protein activation in living cells. Nat. Chem 6, 352–361 (2014). [PubMed: 24651204]

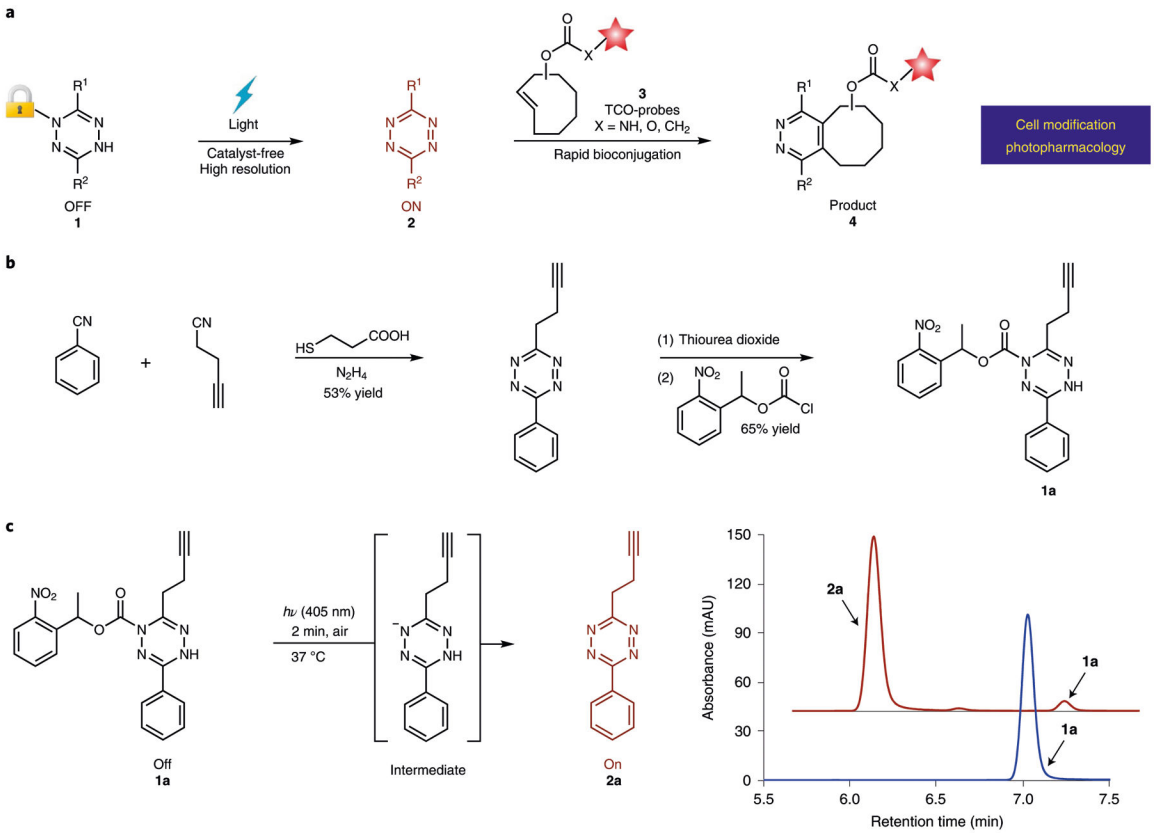

Fig. 1 |. Light-controlled bioorthogonal tetrazine ligation in living cells.

a, Light-activated uncaging of a photoprotected dihydrotetrazine leads to the formation of tetrazine, which reacts rapidly with dienophiles such as tCO. Dienophiles could be appended to fluorescent probes (red star) or uncage prodrugs upon cycloaddition (click to release), enabling applications such as spatiotemporal modification of living cells or photopharmacology. **b**, Synthetic route to photocaged dihydrotetrazine **1a**. **c**, Light-activated formation of tetrazine **2a** from photocaged dihydrotetrazine **1a**. the reaction was carried out by irradiation of photocaged dihydrotetrazine **1a** (16 μm) with an LeD light (405 nm, 18 W) in pBS solution (containing 0.1% DmSO) under open air at 37 °C for 2 min. Samples were taken from the reaction mixture at different time points and examined by HpLC. right: spectra before (blue) and after (red) LeD irradiation for 2 min (absorbance monitored at 280 nm). mAU, milli-absorbance unit.

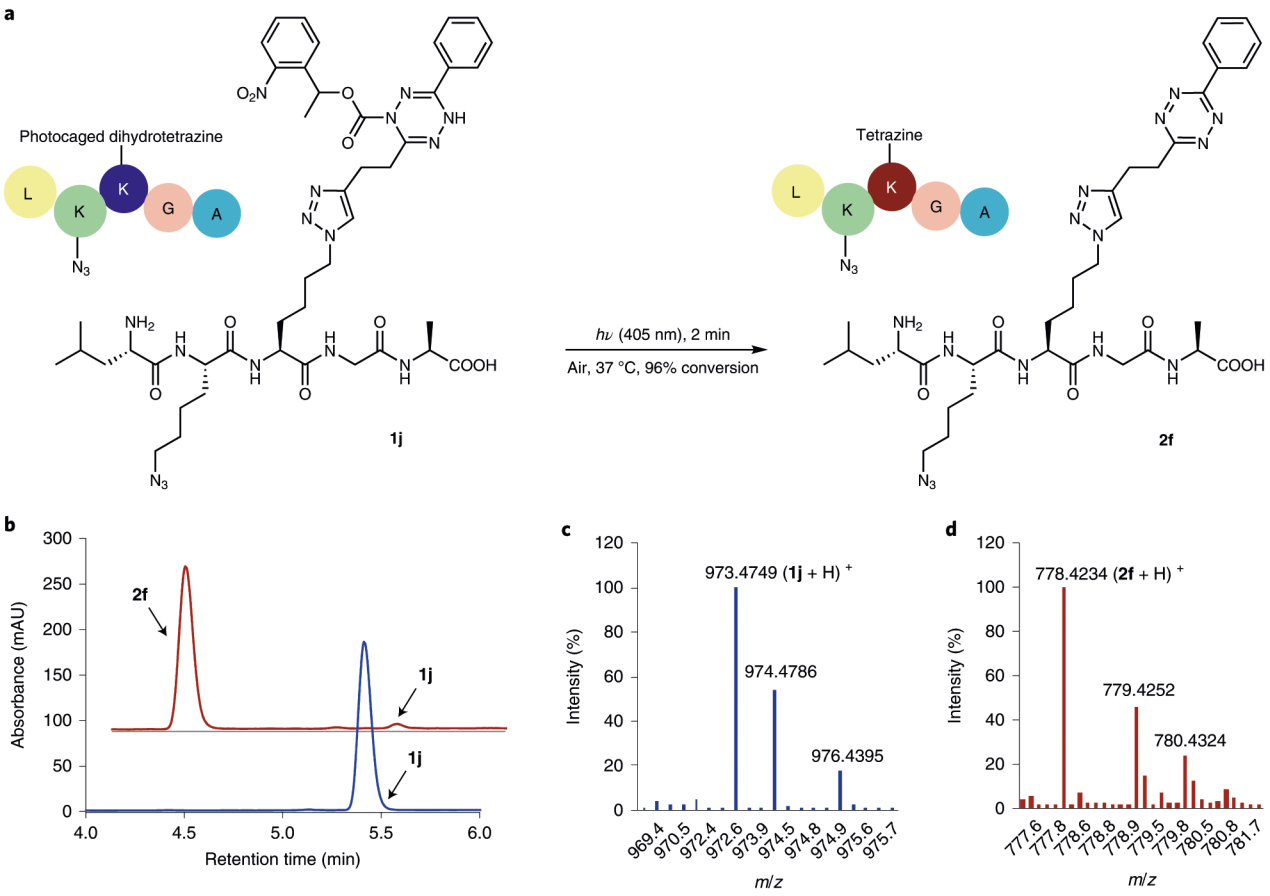

Fig. 2 |. Early-stage functionalization of a peptide with a photocaged dihydrotetrazine group.

a, Light-triggered formation of tetrazine peptide **2f** from peptide **1j**, where a photocaged dihydrotetrazine amino acid was introduced during Fmoc SppS. the reaction was carried out by irradiation of **1j** (10 μm) with LeD light (405 nm, 18 W) in pBS solution (containing 0.2% DmSO and 0.2% DmF) under open air at 37 °C for 2 min. **b**, HpLC/evaporative light scattering detector spectra of the peptide taken before (blue) and after (red) irradiation. **c**, High-resolution mass spectroscopy (HrmS) of photocaged dihydrotetrazine peptide **1j**: expected mass 973.4751 Da, found mass 973.4749 Da. **d**, HrmS results for tetrazine peptide **2f**: expected mass 778.4220 Da, found mass 778.4234 Da.

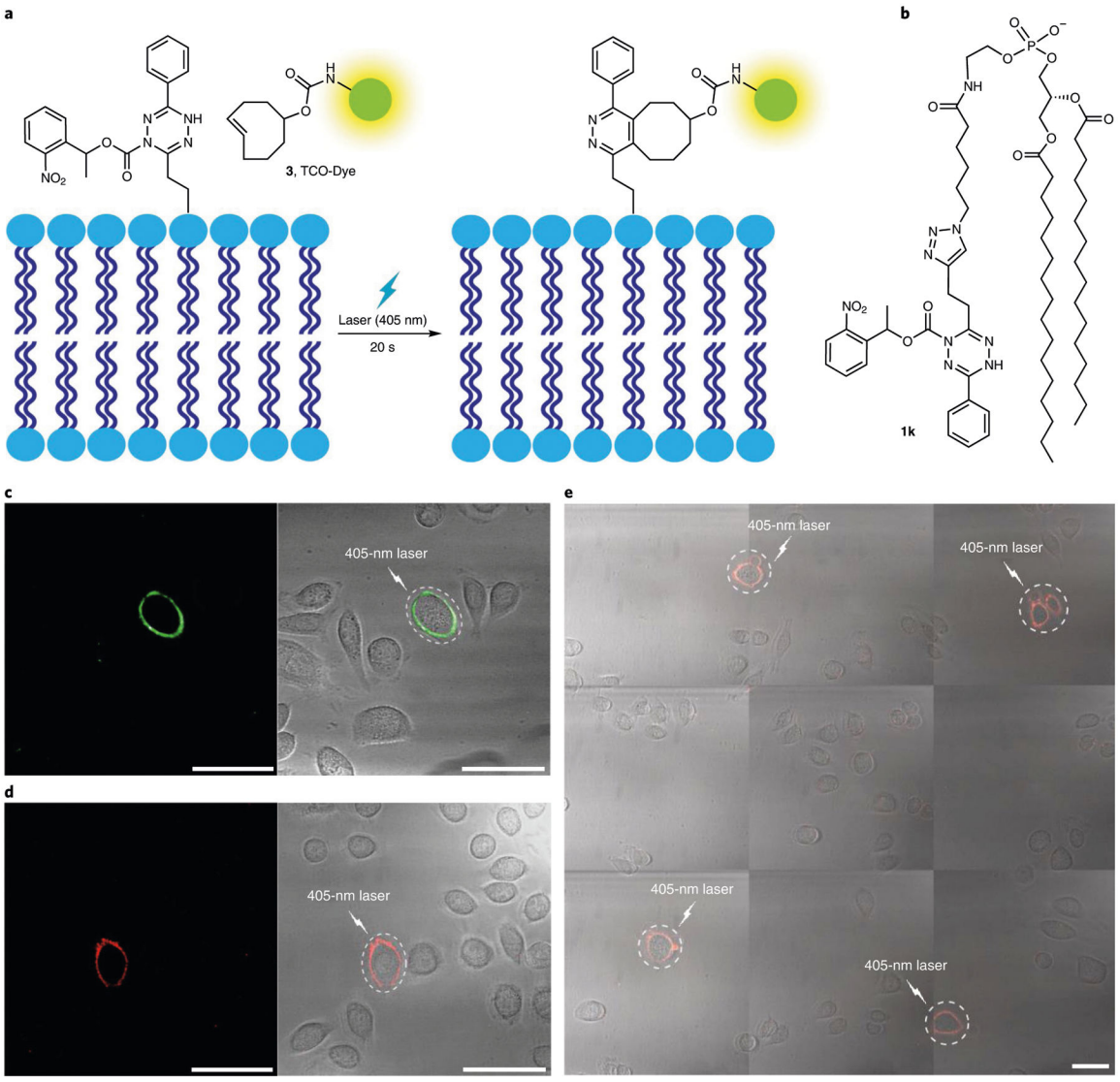

Fig. 3 |. Single-cell remodelling of heLa s3 cell membranes by photoactivation of tetrazine ligation.

a, Cartoon depicting live-cell photoactivation of tetrazine ligation on cellular membranes using photocaged dihydrotetrazine-diacylphospholipid **1k** and a tCO-modified dye (tCO-Dye). **b**, photocaged dihydrotetrazine-diacylphospholipid **1k**. **c**, Fluorescence live-cell labelling demonstrating single-cell photoactivation of tetrazine ligation on the cell membrane of a selected HeLa S3 cell. tCO-AF488 was used for tetrazine ligation. the fluorescence channel (AF488) is shown on the left and merged fluorescence and brightfield channels on the right. the area irradiated by the 405-nm laser is denoted by the white dashed circle. **d**, Single-cell photoactivation of tetrazine ligation on the cell membrane of a selected HeLa S3 cell using tCO-AF568. the fluorescence channel (AF568) is shown on the left and merged fluorescence and brightfield channels on the right. the area irradiated by the 405-nm laser is denoted by the white dashed circle in the merged channel. **e**, Activation of four groups of cells at different locations inside a 0.75 mm by 0.75 mm square area. tCO-AF568 was used for the tetrazine ligation. Images are taken from the merged fluorescence (AF568)

and brightfield channels. the areas irradiated by the 405-nm laser are denoted by white dashed circles. each experiment in **c**–**e** was repeated independently three times, with similar results. Scale bars, 50 μm.

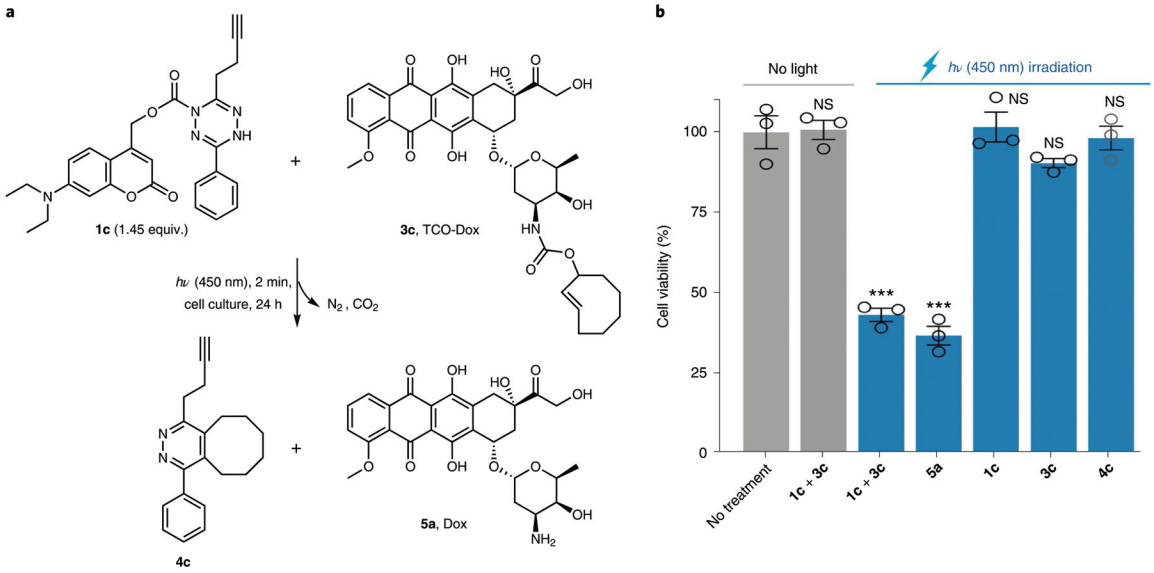

Fig. 4 |. Light-activated tetrazine prodrug therapy in hep 3B cancer cells.

a, Application of light-controlled tetrazine ligation to release the chemotherapeutic doxorubicin in the presence of living Hep 3B cancer cells. Dox, doxorubicin. **b**, Cell viability of Hep 3B cancer cells after treatments with photocaged dihydrotetrazine **1c** (8 μm), tCO-Dox **3c** (5.5 μm), side product **4c** (5.5 μm) and Dox **5a** (5.5 μm), with or without irradiation by LeD light (450 nm, 18 W) for 2 min, followed by incubation at 37 °C for 24 h. Data are presented as mean ± standard error of the mean (s.e.m.), open circles indicate independent experiments ($n = 3$ biologically independent samples). Statistically significant differences in cell viability between no treatment and other treatments are indicated using an independent t-test (two-tailed): ***$P < 0.001$, NS, not significant. Specifically, **1c** + **3c** (450-nm irradiation) versus no treatment: $t = 10.334$, d.f. = 4, $P = 0.000495$; **5a** (450-nm irradiation) versus no treatment: $t = 10.755$, d.f. = 4, $P = 0.000424$.

Table 1 |

Photocaged dihydrotetrazines

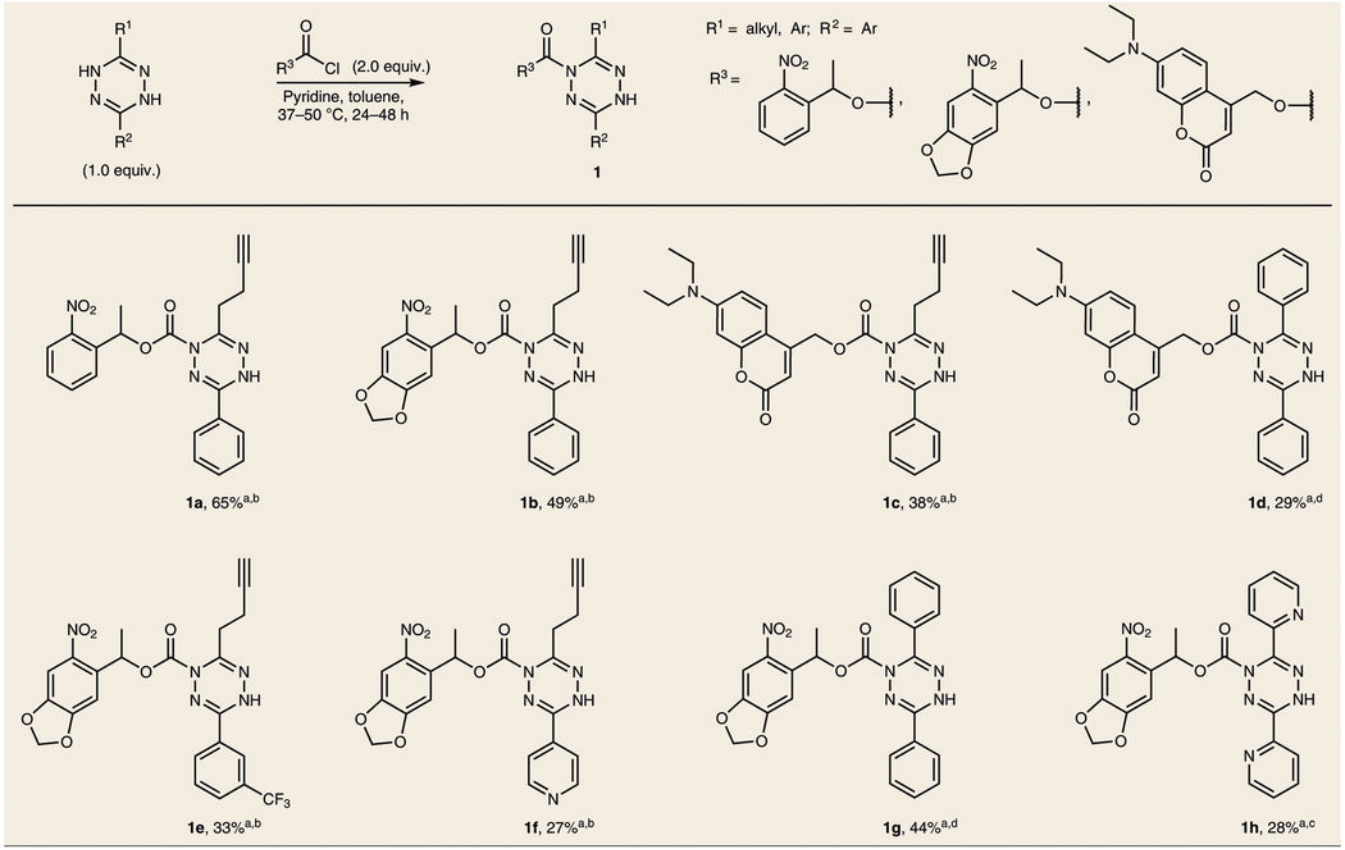

Under argon, anhydrous pyridine was added to dihydrotetrazine (1.0 equiv.) in a sealed flask, followed by slow addition of a solution of photocaged carbonochloridate in toluene (2.0 equiv.) at 0 °C. the reaction mixture was stirred at 37–50 °C for 24–48 h.

[a] Isolated yield.

[b] 37 °C for 24 h.

[c] 37 °C for 48 h.

$d_{50\ °C\ for\ 36\ h.}$